ANALYTIC CALCULATIONS OF HYDRAULIC CONDUCTIVITIES
ABOVE LONGWALL COAL FACES

R.J. Fawcett*, S. Hibberd** and R.N. Singh*

*Department of Mining Engineering,
**Department of Theoretical Mechanics,
University of Nottingham, University Park,
Nottingham, NG7 2RD, United Kingdom.

ABSTRACT

The paper decribes a theoretical investigation into the zones of increased hydraulic conductivity caused by rock failure above a longwall panel. Primitive stresses are determined from empirical expressions and induced stresses are calculated using previously derived analytic formulae. Principal components of the resultant total stress distribution are subjected to Mohr and Griffith failure tests to determine regions of failure. The predictions are illustrated graphically by means of contour diagrams. Predicted failure heights are correlated with existing experimental values and fracture conductivities are investigated by a comparison of theoretical, field and laboratory results.

INTRODUCTION

In many mining circumstances it is of major importance for health, safety and economic reasons to be able to predict the rate of inflow of water to the mine workings. This rate depends crucially on any regions of increased hydraulic conductivity near the mine. The removal of coal by longwall mining methods leads to increases in the hydraulic conductivities of strata above the extraction as a result of fractures extending above the gates, face and start line and by bed separation over the centre of the panel [1, 2]. The two vertical sections of figure 1 illustrate what is generally considered to be the typical behaviour of strata overlying a longwall extraction. The zones of intense fracturing above the edges of the extracted region are usually assumed to be wedge shaped [1, 2].
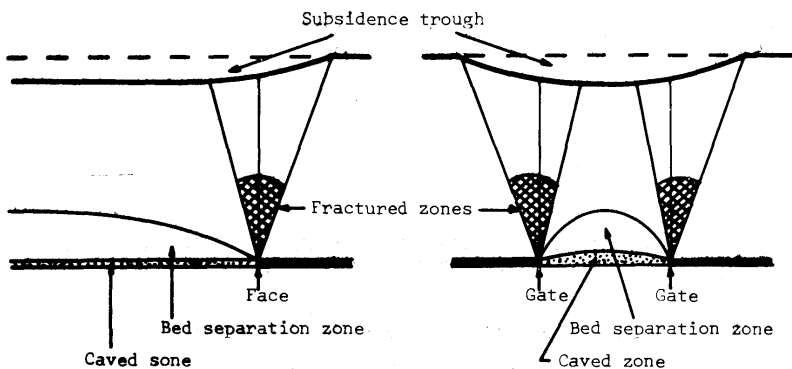
Figure 1   Strata behaviour above a longwall extraction

FIELD INVESTIGATIONS

Field investigations of the changes in hydraulic properties of strata above longwall extractions have concentrated on the height of the fractured zones [1, 3] and on the magnitude of the induced conductivities within and on either side of them [4]. Four empirical equations expressing fracture height as a function of extracted seam thickness have been deduced for different circumstances. The four formulae, and a fifth equation indicating the minimum cover recommended by the National Coal Board of Great Britain when working under the sea [5], are given as:

1) Weak overburden [3] $h = \dfrac{100t}{3.1t + 5.0}$,

2) Medium overburden [3] $h = \dfrac{100t}{1.6t + 3.6}$,

3) Strong overburden [3] $h = \dfrac{100t}{1.2t + 2.0}$,

4) General formula [1] $h = 56\ t^{1/2}$; $0.0 \le t \le 3.5$, and

5) NCB minimum cover [5] $h = 105$; $t \le 1.7$
                              $h = 43t + 32$; $1.7 \le t \le 4.0$

where h is the fracture height or minimum cover as appropriate, t is the extracted thickness and both quantities are given in metres.   In the

case of multiple seam extractions this thickness is the cummulative value. The five relationships are illustrated graphically in figure 2. They show broadly similar trends but there are large differences between the various values of fracture height at any given extraction thickness. An alternative formula $h = 0.83w - 11.0$, based on panel width (w) rather than extraction thickness, predicts greater fracture heights at typical widths between 100 and 200 metres [6].

Figure 2   Fracture height relationships

The magnitudes of induced hydraulic conductivities have been measured by means of pumping-in tests on compartmented boreholes placed above the path of progressing longwall faces [4]. In each experiment measurements were taken at intervals before the arrival of the face, as the face was directly below the borehole and after it passed. Increases in the hydraulic conductivities were first noted between 5 and 10 metres ahead of the face while maximum values were achieved between 20 and 40 metres behind the face. The subsequent decreases in conductivity were more gradual than the increases and undisturbed values were not regained within the duration of the experiments. The results were treated on the assumptions that hydraulic conductivities were anisotropic and that major principal axes were horizontal. The latter assumption was necessary because anisotropic hydraulic conductivities are notoriously difficult to measure, especially under field conditions [7], and the results quoted here did not give the information necessary to determine directions of principal conductivities. On the basis of the assumptions described the horizontal conductivity increased typically from 1.5×10^{-9} ms^{-1} to a maximum value of 6.0×10^{-8} ms^{-1}; an increase of 40 times. The residual conductivity, where measurements ceased at 80 metres behind the face, was between 3.0×10^{-8} ms^{-1} and 4.5×10^{-8} ms^{-1} or 20 to 30 times the undisturbed value.

Numerical calculations of groundwater inflow to longwall coal extractions, based upon the field data described above, have been reported [8]. The mathematical models from which solutions were derived were based upon the simplified cross-section through a longwall face illustrated in figure 3. The coal seam was divided into three parts: an unworked section ahead of the face, an extracted section behind the face and a closed section where roof and floor met further behind the face. Water was assumed to flow through the strata represented within the domain of the model from the aquifer to the extracted part of the seam according to Darcy's Law. The four regions of the model were assigned different anisotropic hydraulic conductivities such that region 1 represented undamaged strata below the seam, ahead of the face and above the highest limit of the fractured zone, regions 2 and 3 represented the fractured zone of maximum conductivity and region 4 represented strata undergoing recompaction in the zone of slightly reduced conductivity behind the face. Solutions of the models demonstrated that the total rate of water inflow to the working was sensitive to the thickness of the intact layer separating the fractured zone from the aquifer, the anisotropic nature of the hydraulic conductivities within the fractured and compacted zones and the degree to which undisturbed conductivities were restored in the compacted zone. The thickness of the intact layer above the fractured zone was critically important, particularly at small thicknesses when the fractured zone approached the aquifer.
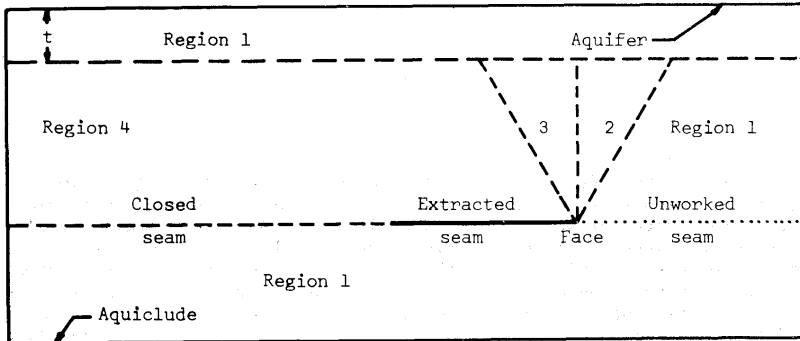

Figure 3   Simplified representation of a longwall face

Coal reserves lying close to heavily waterlogged aquifers or sources of free water will often have to be exploited in the future as more easily worked fields become exhausted. Under these circumstances it will be important to continue working as close as possible to the water sources, until high inflows make operations uneconomic or impractical, in order to avoid unnecessary sterilisation of reserves. Such a requirement will increase the importance of accurate inflow predictions and will make a precise knowledge of the height of the fractured zone under different

physical conditions, and of the hydraulic conductivities associated with it, an imperative necessity. This is particularly so on the basis of numerical results which predicted that the rate of water inflow to a working will increase suddenly once the thickness of the intact layer falls below a critical value [8]. An example of such a dramatic and previously unexpected inrush was to the Wistow Mine in the Selby Coalfield of Great Britain [9].

STRESS ABOVE A LONGWALL PANEL

The extent of the fractured zone, and the directions of anisotropic hydraulic conductivities within it, are determined by the distribution of stress in the overburden. Stresses in strata above a longwall panel have been calculated analytically for a homogeneous transversely isotropic overburden in plane strain cross-section [10]. General solutions were given as distributions of induced stress, defined as the difference between the total stress after excavation and the pre-excavation or primitive stress. Total stress could be found by adding a known or assumed primitive stress distribution. Calculations were based on the assumption that the extracted seam was sufficiently thin compared with the other dimensions of the excavation to be treated as a crack of zero thickness. Closure was represented by a discontinuity in displacement. The excavation was assumed to be horizontal with a width equal to 2a. For the particular solution discussed in this paper the strata sandwiching the coal seam were regarded as being of infinite horizontal and vertical extents. Constant vertical tractions p, equal and opposite to the vertical component of primitive stress at seam level, were applied to the two surfaces of the extraction. The overburden was assumed to possess an axis of transverse isotropy parallel to the vertical (y) direction; elastic constants were defined in terms of the Young's moduli E_x and E_y, the Poisson's ratios ν_x and ν_y, and the shear modulus M.

The solution, a function of x and y co-ordinates originating from the centre of the excavation, gave induced the stresses σ_x, σ_y and τ_{xy} by the complex expressions

$$\sigma_x + \sigma_y = 4 \sum_{j=1}^{2} \{\gamma_j \Omega''(z_j) + \overline{\gamma_j \Omega''(z_j)}\} \tag{1}$$

and

$$\sigma_x - \sigma_y + 2i\tau_{xy} = -4 \sum_{j=1}^{2} \{\gamma_j^2 \Omega''(z_j) + \overline{\Omega''(z_j)}\} \tag{2}$$

where

$$\Omega(z_j) = \frac{\alpha_j}{(\alpha_j - \alpha_{3-j})} H(\xi_j) , \tag{3}$$

$$H'(\xi_j) = \frac{p}{2}\{\xi_j - (\xi_j^2 - a^2)^{\frac{1}{2}}\} , \tag{4}$$

$$\xi_j = \frac{\alpha_j + 1}{2\alpha_j} z_j = x + \frac{iy}{\alpha_j} , \tag{5}$$

$$\gamma_j = \frac{(\alpha_j - 1)}{(\alpha_j + 1)} \tag{6}$$

and the quantities α_1 and α_2 were the two roots of the quartic equation

$$\left\{\frac{1}{E_y} - \frac{\nu_y^2}{E_x}\right\}\alpha^4 + \left\{\frac{2\nu_y(1+\nu_x)}{E_x} - M\right\}\alpha^2 + \left\{\frac{1-\nu_x^2}{E_x}\right\} = 0 \qquad (7)$$

which were either (i) complex conjugates with positive real parts or (ii) real and positive. Physical constraints imposed on the elastic constants ensure that two of the roots of equation (7) always fell into one of these categories.

The assumptions made to enable the analytic solution (1) to (7) to be obtained imposed limitations on the ability of the mathematical model to represent real mining conditions. Firstly, the rock strata were represented as homogeneous, so the heterogeneity which characterises all underground excavations could not be included. However, in a finite element investigation of a similar mathematical model two important heterogeneous features, strong beds and inter-strata lubrication, were shown to be adequately represented by a homogeneous model for the purpose of calculating stress and displacement [11]. The inclusion of the strong strata gave rise to bed separation amounting to about 1% of the seam closure, without altering the general displacement pattern, while the effect of inter-strata lubrication, due typically to thin clay bands, could be obtained by assigning a low shear modulus to a homogeneous model. The bed separation, although mechanically unimportant, would have an effect on water flow. Secondly, the ground was treated as an infinite medium and surface effects were not modelled; this was not a serious limitation when considering the fracture pattern above even moderately deep mines. Thirdly, the calculations were performed on a two dimensional plane strain cross section; consequently three dimensional effects occurring very close to the four junctions of gate with face and gate with start line were excluded. Fourthly, the rock was modelled as a linearly elastic material, thus prohibiting representation of its post-failure characteristics. In the finite element investigation previously quoted it was found that the inclusion of a supposedly failed zone around the extraction, with reduced elastic moduli, had little effect on the general strata deformation [11]. Lastly, the excavation was represented as under constant induced traction; this was equivalent to assuming that the extracted seam was sufficiently thick to prevent the roof and floor from meeting at any point. Thus the stabilising effect of the partial support normally achieved by closure was not included.

Despite these limitations the analytic approach had the important advantage that stress distributions could be reliably obtained from the same general equations (1) to (7) for a wide variety of physical conditions. Alternative numerical schemes, such as the finite element method, can be both time consuming and inaccurate because of their reliance on some type of grid or mesh. The mesh determines the form of the solution and would usually have to be altered between different numerical calculations. It is particularly important to check that pseudo-infinite boundaries are sufficiently remote not to affect results and that regions of high stress gradient are treated with special detail; such a process is often iterative.

PHYSICAL CONSTANTS

A method for determining the elastic constants which enable a heterogeneous rock mass to be represented as a homogeneous transversely isotropic medium has been devised on the basis of stochastic analysis [11]. A random number generator was used to assemble by layers 100 simulated rock masses comprising the constituents of coal measures strata. In each rock mass appropriate elastic constants were assigned to every layer and the equivalent bulk elastic constants calculated. The horizontal and vertical components of Young's modulus and Poisson's ratio were found to be reasonably consistent between different simulated rock masses with mean values given as

	Young's modulus (Nm^{-2})	Poisson's ratio
Horizontal	2.3×10^{10}	0.19
Vertical	1.8×10^{10}	0.22

The vertical Poisson's ratio was calculated according to a definition [11] which differed from another in common use [12] by a factor equal to the ratio of Young's moduli. A Poisson's ratio of 0.17 would be implied by the second definition. The bulk shear modulus was found to be more difficult to calculate because it was heavily dependent upon the degree of inter-strata lubrication; a value of 1.0×10^9 Nm^{-2} was found to be appropriate. These elastic constants were used in the analytic solutions described in this paper.

The primitive stress existing in underground rock masses is generally taken to possess horizontal and vertical ˙principal axes. The vertical component is widely assumed to be due to overburden weight and to have a value proportional to depth [13]. Theoretical considerations of average rock density have given the constant of proportionality as 0.023 $MPam^{-1}$ [14] and 0.025 $MPam^{-1}$ [15]. Empirical results have confirmed the linear nature of the relationship between vertical primitive and depth and have given a multiplying factor of 0.027 $MPam^{-1}$ [13].

The horizontal component of primitive stress has traditionally been taken to be the stress necessary to restrain horizontal deformation [13]. On the basis of the bulk elastic moduli given above the horizontal stress would be 0.27 times the vertical value. In contradiction of this prediction an analysis of 120 measurements of in-situ stress in hard rocks such as quartzite gave horizontal ratios between 0.5 and 4.0 [13]. Other workers have assumed that primitive stress in the softer rocks of the coal measures would become hydrostatic due to creep over geologic time and that vertical and horizontal components would be equal [14, 15]. Consequently all that can be claimed for the horizontal component of primitive stress is that it is not well established.

It has been noted that the induced stress due to longwall mining depends only upon the vertical component of primitive stress at seam level. In many cases, notably when predicting ground deformations and surface subsidence, only the induced stresses and strains are required and the horizontal principal stress is therefore irrelevant [10, 11]. Unfortunately the degree of rock fracture, and the consequent increase in hydraulic conductivity, depends upon the total stress which can be

calculated only if both components of primitive stress are known. On the basis of the preceding discussion the vertical and horizontal primitive stresses σ_y' and σ_x' were taken as

$$\sigma_y' \; [\text{MPa}] \;=\; 0.025 \text{ x depth [metres]} \tag{8}$$

and $$\sigma_x' \;=\; b \text{ x } \sigma_y' \tag{9}$$

where the primitive stress ratio b could have any positive value up to 4.0. It will be shown that the precise value of this ratio is of crucial importance in determining the regions of fracture above longwall excavations.

ROCK FRACTURE

A substantial critical review of the major theories of brittle fracture in rock has been published [16]. In each theory an attempt is made to determine a failure envelope, in the form of a direct or indirect relationship between the maximum and minimum principal stresses σ_1 and σ_2, such that rock will remain intact if the two stresses lie on one side of the envelope and will fail if they lie on the other. The two most accepted relationships are Mohr's criterion and Griffith's theory. Mohr's approach was to derive failure envelopes experimentally for different rock types, without attempting to match them to any theory. Griffith deduced a mathematical relationship for the fracture stresses on the assumption that failure occurred by the propogation of randomly orientated microscopic cracks already existing in nominally intact rock. Griffith's theory predicts a parabolic Mohr envelope which might apply to sedimentary rocks, such as limestone, sandstone and carbonaceous, but which does not describe correctly more brittle rocks like granite and quartzite.

When failure occurs under two compressive principal stresses, represented as positive according to the usual rock mechanics convention, the empirical Mohr approach is usually adopted. The failure criterion is given as a graphical relationship between normal and shear stresses, but under many circumstances it is possible to represent it approximately by the linear expression involving principal stresses

$$\sigma_1 \;=\; C_o \;+\; k\,\sigma_2 \tag{10}$$

where C_o is the unconfined compressive strength and k is the triaxial stress factor. The factor k takes a typical value of 4 for coal and the average coal measures rocks, indicating that their compressive strengths increase substantially with confining pressure [15].

Extrapolation of the Mohr curve to conditions where one principal stress (σ_2) is tensile does not predict failure correctly [16]. However it is clear that failure under tension is of particular importance in determining regions of increased hydraulic conductivity above a longwall excavation. The Griffith theory applies to tensile as well as compressive failure and leads to the failure relationship

$$(\sigma_1 - \sigma_2)^2/(\sigma_1 + \sigma_2) \;=\; 8T_o \qquad \sigma_2/\sigma_1 > -0.33$$

or $$\sigma_2 \;=\; -T_o \qquad \sigma_2/\sigma_1 \leq -0.33$$

where T_o is the unconfined tensile strength. Thus if stresses σ_1 and σ_2

are compressive and tensile respectively, such that

$$\sigma_1 = -m\sigma_2, \tag{11}$$

then tensile failure will occur, according to the Griffith theory, when

$$\sigma_2 = -cT_o \tag{12}$$

where $\qquad c = 8(m - 1)/(m + 1)^2 \qquad m > 3 \tag{13}$

or $\qquad c = 1 \qquad m \leq 3. \tag{14}$

The Griffith criterion implies that the effect of a confining stress is to decrease the tensile strength or leave it unchanged, depending upon the relative magnitude of the two principal stresses. The alternative Mohr aproach is to assume that tensile failure will occur only when the unconfined tensile strength is exceeded, which is equivalent to adopting equation (14) for all values of m.

Unconfined compressive strengths determined in the laboratory for typical coal measures rocks ranged from 40 to 70 MPa, while unconfined tensile strengths lay between 2.5 and 5.7 MPa [17]. In-situ strengths are substantially smaller than laboratory values because rock masses contain joints, fractures and other planes of weakness which are deliberately excluded from core samples selected for testing. It has been proposed that laboratory determined unconfined compressive strengths should be reduced by a factor lying between 1 and 7, dependent upon rock type, to give in-situ strengths [15]. It is clear that in-situ tensile strengths must also be reduced.

The arguements discussed above suggest that compressive rock failure is determined, on the basis of equation (10) and the subsequent discussion, by a parameter which will be defined as

$$\text{modified compressive stress} = \sigma_1 - 4\sigma_2 \tag{15}$$

while tensile failure is affected, according to equations (11) to (14), by a second parameter defined as

$$\text{modified tensile stress} = \frac{\sigma_2}{c}. \tag{16}$$

The two modified stresses of equations (15) and (16) can be compared directly to the two in-situ unconfined compressive and tensile strengths in order to asses regions of failure.

CALCULATED STRESS AND INDUCED FAILURE

Calculations of induced stress were performed, using equations (1) to (7), for a longwall extraction with a width (a) equal to 100 metres and an imposed traction (p) equal to 12.5 MPa, the latter corresponding to a depth of 500 metres. Total stress distributions were obtained by superimposing various primitive stresses, calculated according to equations (8) and (9), with the ratio b taking values between 0.25 and 1.0. Contour diagrams were generated to illustrate the distributions of the modified stresses defined in equations (15) and (16) and the unmodified tensile stress σ_2. On the basis of typical unconfined strengths already noted, and bearing in mind the in-situ strength

reduction, compressive contours were plotted between 20 and 50 MPa (although the higher contours were often absent) while tensile contours filled the range 1 to 6 MPa.

Figures 5 and 6 show the contours obtained for principal stress ratios of 0.25 and 0.5. In each case compressive failure occurred over the rib pillar or front abutment zone while tensile failure was restricted to strata above the panel. The tensile diagrams include short straight lines parallel to the principal stress σ_1 showing the orientation of fractures induced by failure.

Figure 5 illustrates particularly clearly two separate zones of tensile failure: one induced by strata bending immediately behind the face, and extending approximately vertically, and the other caused by the roof stretching over the whole of the panel. The zone of bending appeared only in the modified tensile stress diagram while the more limited zone of stretching was predicted identically by the modified and unmodified tensile stress distributions. In figure 4 the two zones merged and were present in both diagrams; however that part of the failure region which was due mainly to bending was more extensive in the modified stress diagram. In each of figures 5 and 6 the failure height implied by the modified tensile stress was approximately the same as that predicted by a consideration of the modified compressive stress.

It is clear that once rock has failed under compression then its resistance to tensile stress will be reduced. The stress diagrams of figures 4 and 5 therefore suggest that rock failure is initiated by the high compressive stresses ahead of the face with the resultant fractures being subsequently opened by tensile strains developing in the failed rock behind the face. This is consistent with the experimental observation already noted, that hydraulic conductivity begins to increase between 5 and 10 metres ahead of the face and reaches a maximum between 20 and 40 metres behind it [4]. The measured distances support the predictions of figure 4, where the primitive stress ratio was 0.25, in preference to those of figure 5. The precise appearance of each diagram is partly governed by the particular choice of contours and the inclusion of lower values of compressive and tensile stress, indicating the limits of failure in weaker rock, would alter the relative credibility of the two diagrams.

FRACTURE CONDUCTIVITY

Laboratory measurements have shown that the hydraulic conductivities of fractured coal and coal measures rocks are fairly independent of the nature of the rocks or their undamaged hydraulic conductivities [18]. Fracture conductivities of coals have been determined to lie in the range 10^{-7} to 10^{-6} ms^{-1}, typically 4×10^{-7} ms^{-1}, for unconfined samples. They decreased approximately logarithmically with confining stress, to between 1/3 and 1/10 of unconfined values at radial and axial stresses of 3 and 8 MPa respectively [19]. Information about fracture conductivities under tensile stress was not available because of the difficulty of maintaining failed samples intact.

The field measurements of hydraulic conductivities above a longwall panel already mentioned indicated that the maximum value attained was 6×10^{-8} ms^{-1} [4]. This was determined by treating flow figures from vertical boreholes on the assumption that the major principal conductivity was horizontal [4]. Figures 4 and 5 demonstrate that the assumption was
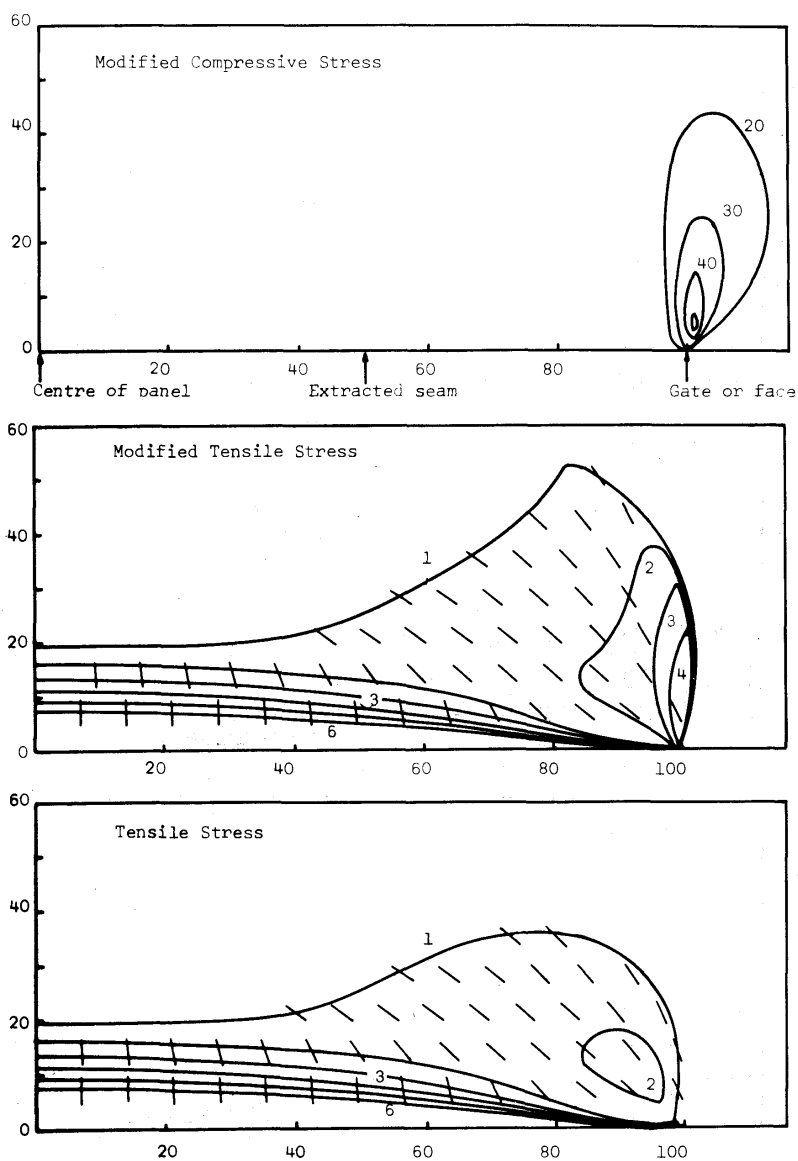
Figure 4 Principal stress contours (MPa) for primitive stress ratio 0.25 (distances in metres)
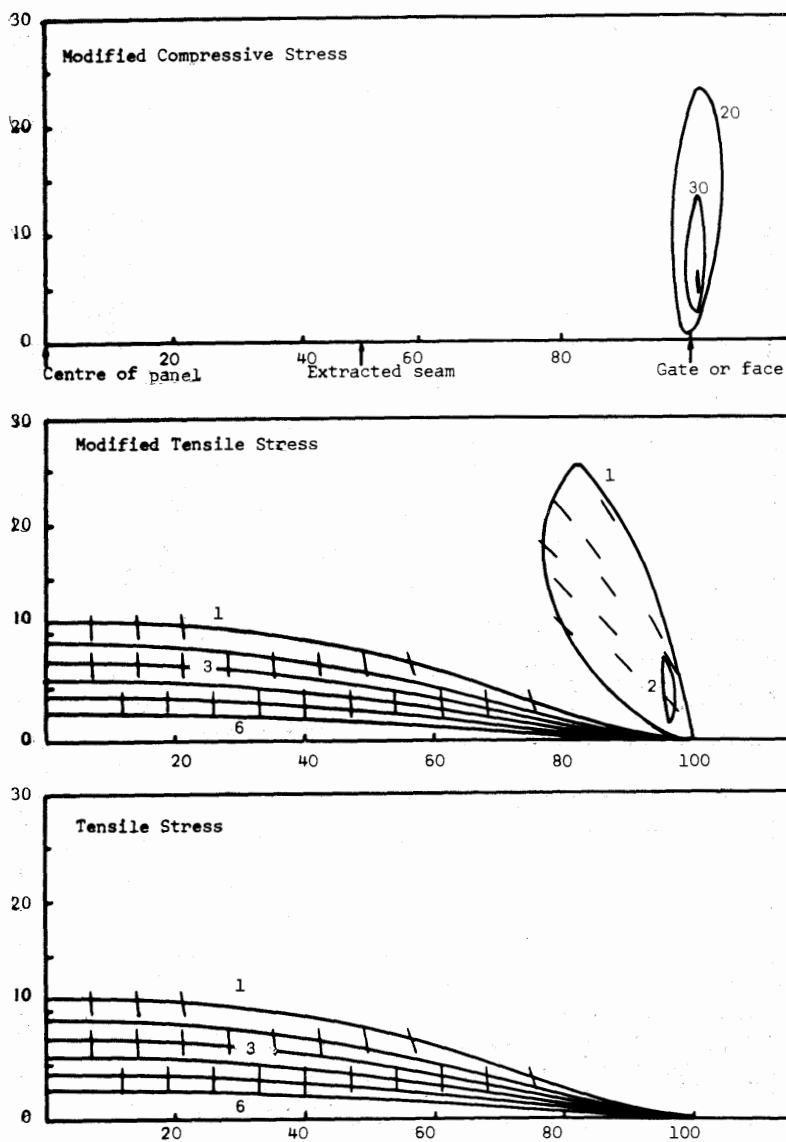
Figure 5 Principal stress contours (MPa) for primitive stress ratio 0.5
(distances in metres)

probably incorrect and that in consequence the major principal conductivity was under-estimated. The true value would thus have been closer to the unconfined values obtained in the laboratory [19].

FRACTURE HEIGHTS

Figures 4 and 5 indicate the strong dependence of compressive and tensile failure heights upon the ratio of horizontal to vertical primitive stress. The reason for such dependence is that a larger horizontal principal stress increases compressive strength, according to equation (10), in regions prone to compressive failure, while decreasing tensile stresses, by simple addition of a larger compressive stress, in regions prone to tensile failure. In both cases the failure height is reduced by a half when the principal stress ratio is changed from 0.25 to 0.5.

In order to further investigate the dependence of fracture height upon the horizontal primitive stress, contour diagrams were generated in more detail for six values of the primitive stress ratio. The maximum heights at which different modified compressive and tensile stresses were achieved are indicated in table 1.

Stress ratio b	Compressive failure heights (m)			Tensile failure heights (m)		
	20MPa	30MPa	40MPa	1MPa	2MPa	3MPa
0.25	45.0	25.0	15.0	53.0	37.0	29.0
0.375	32.0	19.0	11.0	35.0	23.5	15.0
0.5	23.5	13.5	7.5	26.0	11.0	1.0
0.625	17.0	10.0	5.5	20.5	4.0	1.0
0.75	12.0	7.0	4.0	–	–	–
1.0	1.7	0.8	0.0	–	–	–

Table 1. Failure heights for different primitive stress ratios

Tensile failure heights ceased to be recorded beyond a principal stress ratio of 0.625 because of the appearance of a new phenomenon: at a ratio of 0.75 the tip of the zone of bending expanded into a much larger zone where the high horizontal stress combined with a small but nearly vertical tensile stress to cause failure along horizontal fractures. The zone, which might be taken to represent bed separation, extended to a maximum height of over 100 metres above the centre of the panel but did not reach down to the worked seam at any point other than by its connection with the bending zone. The principal stress ratio at which the effect first manifested itself depended upon the smallest tensile contour selected: at 0.7 MPa the bed separation zone appeared at a ratio of 0.5. The phenomenon is probably not physically realisable because in practice the worked seam would close and support the overlying strata, thus removing or reducing vertical tension. The analytic solution is valid chiefly for the region above the face and an iterative numerical scheme is currently under development to investigate, among other concerns, the effects of closure.

Table 1 clearly demonstrates that the height of rock failure decreases substantially with increasing primitive stress ratio, whether

compressive or tensile stress is considered, and that failure is negligible at a hydrostatic primitive stress. In general the decline is more rapid for tensile stress than for compressive. The results of table 1 are illustrated graphically in figure 6 which shows failure height as a function of the primitive stress ratio for each of the six stress values.
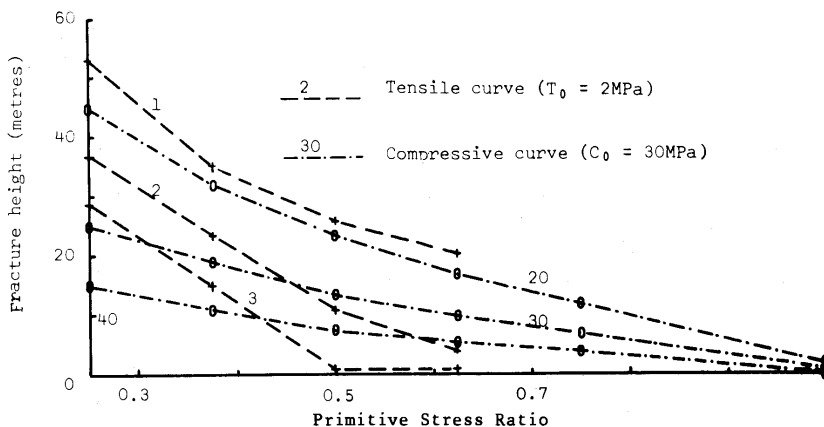

Figure 6   Fracture heights for different tensile and compressive strengths

CORRELATION WITH EMPIRICAL FORMULAE

The analytic solution discussed in this paper gave a maximum vertical roof displacement of 0.275 metres at the centre of the extracted panel. Because of the symmetry of the model an opposite displacement is obtained at the floor, so the closure is equal to 0.55 metres. The ratio of seam closure to extracted seam height is always less than one because of the expansion of broken rock: values of 0.38, 0.475 and 0.84 have been proposed [11]. The middle of these three implies that the closure of 0.55 metres would correspond to an extraction height of 1.2 metres. A thinner seam would allow partial roof support, leading to less strata damage than predicted, while a thicker seam would allow substantial collapse as a result of failure, leading to extension of the analytically modelled zones of damage.

Applying a seam height of 1.2 metres to the empirical formulae illustrated in figure 2 gives predicted fracture heights of 13.8, 21.7, 34.9 and 61.3 metres. These values are of the same order of magnitude as those predicted analytically. Inspection of figure 6 suggests that the primitive stress ratio cannot be greater than 0.625 and that a value nearer to 0.25 is more likely to be correct. The latter corresponds to the old assumption that the horizontal primitive stress in rock strata is that required to restrain lateral deformation [13].

58

CONCLUSIONS

The authors have calculated total stress distributions above a longwall panel using a previously derived analytic solution for induced stress and empirical formulae for primitive stress. Mohr and Griffith failure criteria have been applied to predict zones of fracture which have then been correlated with experimental results. The extent of failure has been shown to be highly sensitive to the ratio of horizontal to vertical primitive stress, a quantity about which existing knowledge is poor. Variation in field values of the ratio may explain the difficulty in predicting failure heights accurately. The calculations described in this paper suggest that a ratio of 1.0, corresponding to the assumption of hydrostatic stress, is probably not correct and that the smaller plane strain value would be more appropriate. Qualitative interpretation of the calculated results supports the view that rock failure leading to increased hydraulic conductivity is initiated by high compressive stresses ahead of the face and that the fractures are subsequently opened by tensile stresses behind the face.

The analytic approach has certain limitations; consequently finite element work is currently being undertaken to investigate the effects on the predicted failure zone of seam closure, stress re-distribution due to rock failure, and proximity of the ground surface. This will be the subject of a forthcoming paper.

ACKNOWLEDGEMENTS

REFERENCES

1. Singh M.M. and Kendorski F.S.
   Strata disturbance predictions for mining beneath surface water and waste impoundments
   Proc. 1st Ann. Conf. Ground Control in Mining, Univ. West Virginia, July 1981

2. Singh R.N. and Atkins A.S.
   Design considerations for mine workings under accumulations of water
   Int. J. Mine Water, vol 1, no 4, Dec 1981

3. Chuen L.T.
   Practice and knowledge of coal mining under water bodies
   10th World Mining Congress, Istanbul, 1979

4. Whittaker B.N., Singh R.N. and Neate C.J.
   Effect of longwall mining on ground permeability and subsurface drainage
   1st Int. Mine Drainage Symp., Denver, 1979

5. National Coal Board
   Working under the sea
   NCB Mining Department Instruction PI/1968/8 (Revised 1971)

6. Farmer I.W.
   Private communication, 1980

7. Rice P.A., Fontugne D.J., Latini R.J. and Barduhn A.J.
    Anisotropic permeability in porous media
    Flow through porous media [ed. R. Nunge], p47, Am. Chem. Soc.,
    Washington, 1970

8. Singh R.N., Hibberd S. and Fawcett R.J.
    Numerical calculation of groundwater inflow to longwall coal faces
    Proc. 2nd Int. Mine Water Con., IMWA, Granada, 1985

9. The Times
    Pitting their wits against water
    24th August 1983

10. Berry D.S. and Sales T.W.
    An elastic treatment of the ground movement due to mining - II:
    transversely isotropic ground
    J. Mech. Phys. Solids, vol. 19, pp52-62, 1961

11. Shippam G.K.
    Numerical investigation of elastic behaviour around longwall
    excavations
    PhD thesis, Univ. of Nottm., 1969

12. Zienkiewicz O.C.
    The Finite Element Method [3rd ed.]
    McGraw-Hill, England, 1977

13. Brown E.T. and Hoek E.
    Trends in relationships between measured in-situ stresses and depth
    Int. J. Rock Mech. Min. Sci., vol. 15, pp211-215, 1978

14. Berry D.S.
    Ground movement considered as an elastic phenomenon
    Mining Engineer, vol. 123, no. 37, 1963

15. Wilson A.H.
    The stability of underground workings in the soft rocks of the coal
    measures
    PhD thesis, Univ. of Nottm., 1980

16. Obert L.
    Brittle fracture of rock
    Fracture [ed. H. Liebowitz], vol.7, pp93-155, Academic Press, 1972

17. Muftuoglu Y.V.
    A study of factors affecting diggability in British surface coal mines
    PhD thesis, Univ. of Nottm.

18. Mordecai M.
    An investigation into the effect of stress on the permeability of rock
    taken from carboniferous strata
    PhD thesis, Univ. of Nottm., 1971

19. Durucan S.
    An investigation into the stress-permeability relationship of coals
    and flow patterns around working longwall faces
    PhD thesis, Univ. of Nottm., 1981